scientific reports

Check for updates

OPEN

Trabeculae microstructure parameters serve as effective predictors for marginal bone loss of dental implant in the mandible

Hengguo Zhang[1,2,3], Jie Shan[1,2,3], Ping Zhang[2], Xin Chen[1,2] & Hongbing Jiang[1,2]✉

Marginal bone loss (MBL) is one of the leading causes of dental implant failure. This study aimed to investigate the feasibility of machine learning (ML) algorithms based on trabeculae microstructure parameters to predict the occurrence of severe MBL. Eighty-one patients (41 severe MBL cases and 40 normal controls) were involved in the current study. Four ML models, including support vector machine (SVM), artificial neural network (ANN), logistic regression (LR), and random forest (RF), were employed to predict severe MBL. The area under the receiver operating characteristic (ROC) curve (AUC), sensitivity, and specificity were used to evaluate the performance of these models. At the early stage of functional loading, severe MBL cases showed a significant increase of structure model index and trabecular pattern factor in peri-implant alveolar bone. The SVM model exhibited the best outcome in predicting MBL (AUC = 0.967, sensitivity = 91.67%, specificity = 100.00%), followed by ANN (AUC = 0.928, sensitivity = 91.67%, specificity = 93.33%), LR (AUC = 0.906, sensitivity = 91.67%, specificity = 93.33%), RF (AUC = 0.842, sensitivity = 75.00%, specificity = 86.67%). Together, ML algorithms based on the morphological variation of trabecular bone can be used to predict severe MBL.

Peri-implant bone tissue is fundamental for the initial stability and long-term survival of dental implants, and marginal bone resorption around the implant could result in implant failure[1,2]. Currently, acceptable standards of implant success are defined as marginal bone loss (MBL) less than 1.5–2.0 mm after the first year of functional loading and subsequently less than 0.2 mm per year[3–5]. Although radiographic assessment of MBL has been considered as an authoritative criterion to evaluate implant success[3,6], how to predict MBL remains unclear. Therefore, it is urgent to find an effective method to predict MBL and the survival rates of implants.

It has been widely acknowledged that MBL is a multicausal condition with different risk factors playing their roles simultaneously[7,8]. At the early post-loading stage, occlusal force transmits through the implant to the alveolar bone and promotes bone remolding. Plenty of morphology parameters can exhibit the morphological and mechanical properties of trabecular bone in this process[9–11]. Other factors that might impact bone remolding or MBL include the configuration of the dental implant[9,12], cortical bone thickness[10], periodontal disease susceptibility[13], and smoking[14]. Some researchers have employed linear model to predict MBL based on bone structure parameters with sensitivity of 62.1% and specificity of 67.5%[15]. Hence, the establishment of a precise model to predict MBL is still a challenging exploration.

Machine learning (ML) can utilize statistical and optimization techniques to learn and detect in-depth relationships from complex and large data sets[16]. ML has already been applied in many aspects of the medical domain, including disease detection, diagnosis, and treatment[17–19]. Notably, prognosis prediction of dental implant which based on ML model has been applied in several clinical research[20,21]. These results prompt us to investigate whether ML models can predict MBL more accurately than conventional statistical methods.

This study aimed to find an effective way to predict the occurrence of MBL. We hypothesized that ML algorithms combined with clinical and CBCT data could predict MBL more accurately than conventional methods. Four ML models, including Support Vector Machine (SVM), Artificial Neural Network (ANN), Logistic

[1]Jiangsu Key Laboratory of Oral Diseases, Nanjing Medical University, No. 136, Hanzhong Road, Nanjing 210029, Jiangsu Province, China. [2]Department of Oral and Maxillofacial Surgery, The Affiliated Stomatological Hospital of Nanjing Medical University, Nanjing 210029, Jiangsu Province, China. [3]These authors contributed equally: Hengguo Zhang and Jie Shan. ✉email: jhb@njmu.edu.cn

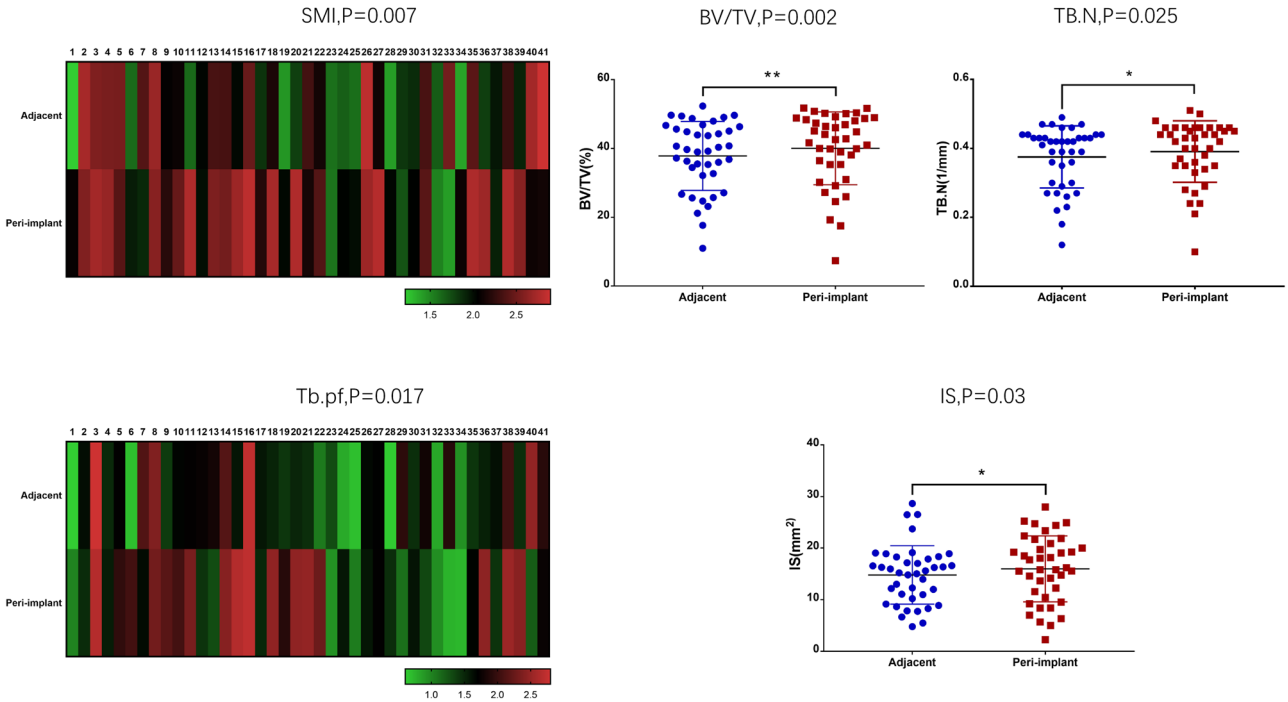

Figure 1. Comparison of morphological parameters among the peri-implant and normal adjacent alveolar bone in cases and controls. In severe MBL cases, SMI and Tb.Pf showed the visible difference between the peri-implant and normal adjacent alveolar bone. BV/TV, Tb.N, and i.S exhibited a significant difference between the peri-implant and normal adjacent alveolar bone in normal controls.

Regression (LR), and Random Forest (RF), were employed to predict MBL. ML models showed superior performance compared to the single predictor in predicting MBL of mandibular implant.

Results

Trabecular microarchitecture changes in severe MBL cases. Eighty-one subjects were included in this study, and 41 were identified severe MBL of dental implants. Gender (P = 0.007), cortical bone thickness (P = 0.007), and smoking (P = 0.008) showed a significant difference between the severe MBL cases and the normal controls (Supplementary Table S1). Morphological variables of the peri-implant and the normal adjacent alveolar bone were also compared between the severe MBL cases and the normal controls. Structure model index (SMI) (P = 0.007) and trabecular pattern factor (Tb.Pf) (P = 0.017) significantly increased in peri-implant alveolar bone of severe MBL cases (Fig. 1). Percent bone volume (BV/TV) (P = 0.002), trabecular number (Tb.N) (P = 0.025), and intersection surface (I.S) (P = 0.030) significantly increased in peri-implant alveolar bone of normal controls (Fig. 1). Additionally, we analyzed preoperative trabecular microarchitecture parameters of all subjects at T_0, and there was no difference between the two groups. The results of trabecular microarchitecture variables at T_1 and T_0 was exhibited in Supplementary Tables S2 and S3.

Morphological variables and their role in predicting MBL. Inspired by the above findings, we analyzed all variables using principal component analysis and correlation covariance matrices. All results relevant to morphological variables were confirmed with a significant difference and reasonable collinearity. SMI, Tb.Pf, Tb.N, bone surface volume ratio (BS/BV), and BV/TV manifested a higher correlation with MBL, while other morphological variables could not bring a noteworthy contribution. Figure 2 reflected the ordination and contribution of all variables, along the first two "Multiple Factor Analysis" (MFA) components. The components explained 47.2% of the total variance in the data. Morphological parameters located in component 1 made significant contributions to the principal component, and all clinical parameters distributed in component 2.

The logically obvious correlation between morphological parameters was shown in Fig. 3, and almost all correlation coefficients reached remarkably significant levels. Meanwhile, the linearity and credibility of trabecular bone microparameters were verified. SMI (P = 0.002) and Tb.Pf (P = 0.0165) exhibited a significantly high positive correlation with MBL. However, BV/TV and BS/BV manifested a negative correlation with MBL. Gender (P = 0.007), cortical bone thickness (P = 0.0072), and smoking (P = 0.0079) were powerfully correlated with MBL.

Performance of ML models. Based on the consequence of correlation analysis, we eliminated some meaningless variables to build ML models. Each model was superior to a single factor predictor. The SVM model performed the best (AUC = 0.967), followed by ANN (AUC = 0.928), LR (AUC = 0.906), RF (AUC = 0.842), SMI alone (AUC = 0.705), Tb.Pf alone (AUC = 0.663), and BV/TV alone (AUC = 0.629) (Fig. 4, Table 1). As the best

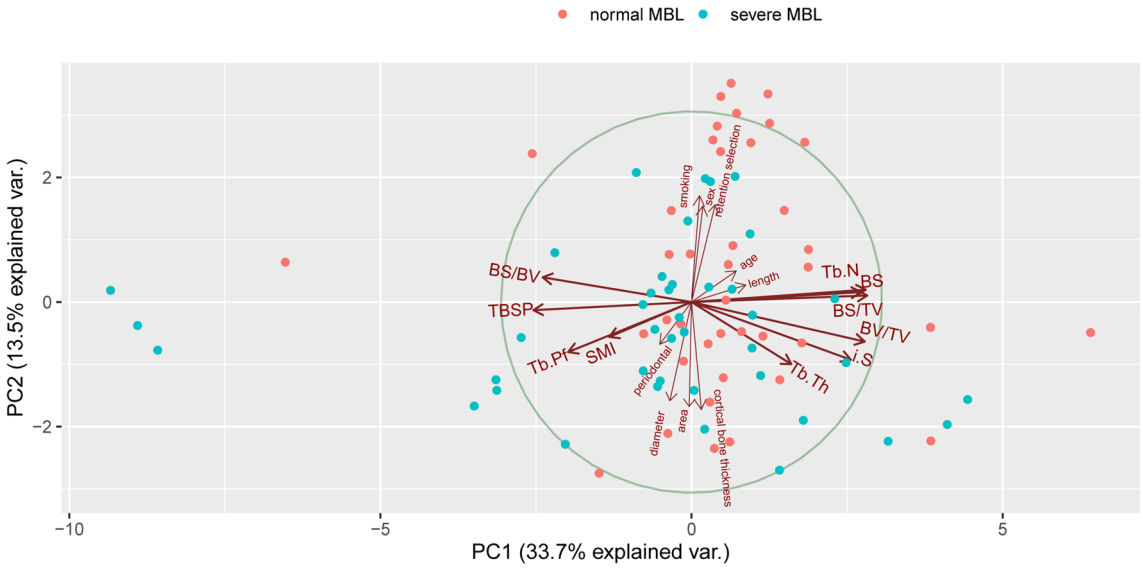

Figure 2. Plots of all variables in MFA. Closely clustered variables were positively correlated, while variables in opposing directions were negatively correlated. The length of the vector represented the importance of the variable in the MFA. Variables close to the midpoint of the circle plot had low contribution and weightage in the projection.

model, the SVM's sensitivity and specificity were 91.67% and 100.00% at its optimal cutoff, respectively. SVM also presented a perfect optimal criterion (0.917), satisfied positive (1.000) and negative (0.938) predictive values, the maximum positive diagnose-likelihood-ratio (Infinite), and the minimum negative diagnose-likelihood-ratio (0.083). Moreover, the SVM model had the smallest false positivity and false negativity. The cutoff value of SMI was 1.027, while the corresponding sensitivity and specificity were 65.85% and 67.50%, respectively. The cutoff value of Tb.Pf was 0.968, and the sensitivity and specificity were 63.41% and 62.50%, respectively. We listed the performance of each model in Table 2. Based on the RF model, we rearranged the variables according to the importance of predicting MBL measurement through the Gini index (Fig. 5).

Discussion

Due to the important role of MBL in dental implant failure, MBL have become an essential clinical examination in postoperative follow-up. The purpose of this study was to verify that ML algorithms combined with early-stage trabecular bone variables could predict MBL more effectively than conventional methods. Our results showed a great performance of ML methods for predicting MBL, which can be considered as the feasible early warning for severe MBL. It was noted that the other factors resulting in MBL should be taken into account in future studies.

Previous researches about MBL mainly concentrated on the cause and treatment[6,9,12,13,22,23], but rarely on the prediction of MBL[15]. Factors such as trabecular bone microstructure parameters possibly affecting MBL during bone remolding have been well elucidated[15], but the role of trabecular bone in this progression remains unclear. To our knowledge, this is the first study to establish and validate ML models based on trabecular microstructure parameters to predict the occurrence of MBL of the submerged dental implant in mandible.

It has been widely acknowledged that various factors, including cortical bone thickness, smoking, periodontitis, SMI, Tb.Pf, and BV/TV, function as a complex to cause MBL[8]. Previous studies have also demonstrated that the proportion of cancellous bone[10], crown-to-implant ratio[24], bone texture, and cortical width[15], are risk factors of MBL. Therfore, single predictive factor cannot accurately predict MBL because MBL is a multifactorial outcome. One recent study attempted to employ Cox regression and mixed linear modeling to predict the occurrence of MBL, but they aimed to assess interventions and their consequences with regard to further bone loss at sites diagnosed with peri-implant inflammation[25]. Another study incorporated several radiographic features of cortical and cancellous bone texture, cortical width, and patient smoking habits to build a statistical model to predict MBL with a sensitivity of 62.1% and specificity of 67.5%[15]. Compared to conventional statistical methods, the current study verified that ML algorithms predicted MBL more accurately. Of note, the SVM model performed best with a sensitivity of 91.67% and specificity of 100.00%, which was significantly better than that of SMI, Tb.Pf or BV/TV alone.

To demonstrate the differences and correlations of morphological variables between the controls and severe MBL cases, we also analyzed morphological variables of trabecular bone in patients with MBL during bone remolding. At the early stage of functional loading, CBCT analysis exhibited a worse outcome of SMI and Tb.Pf in peri-implant alveolar bone of severe MBL cases. These findings revealed that severe MBL cases demonstrated the premonitory morphological variation in trabecular microarchitecture at the early stage. Consistent with our results, a previous study reported that the preservation and improvement of trabecular microarchitecture always brought about a better therapeutic benefit for osteoporosis at multiple skeletal sites[26]. SMI and Tb.Pf were the best determinants of the MBL level, which they reflected the structure quality of the trabecular bone

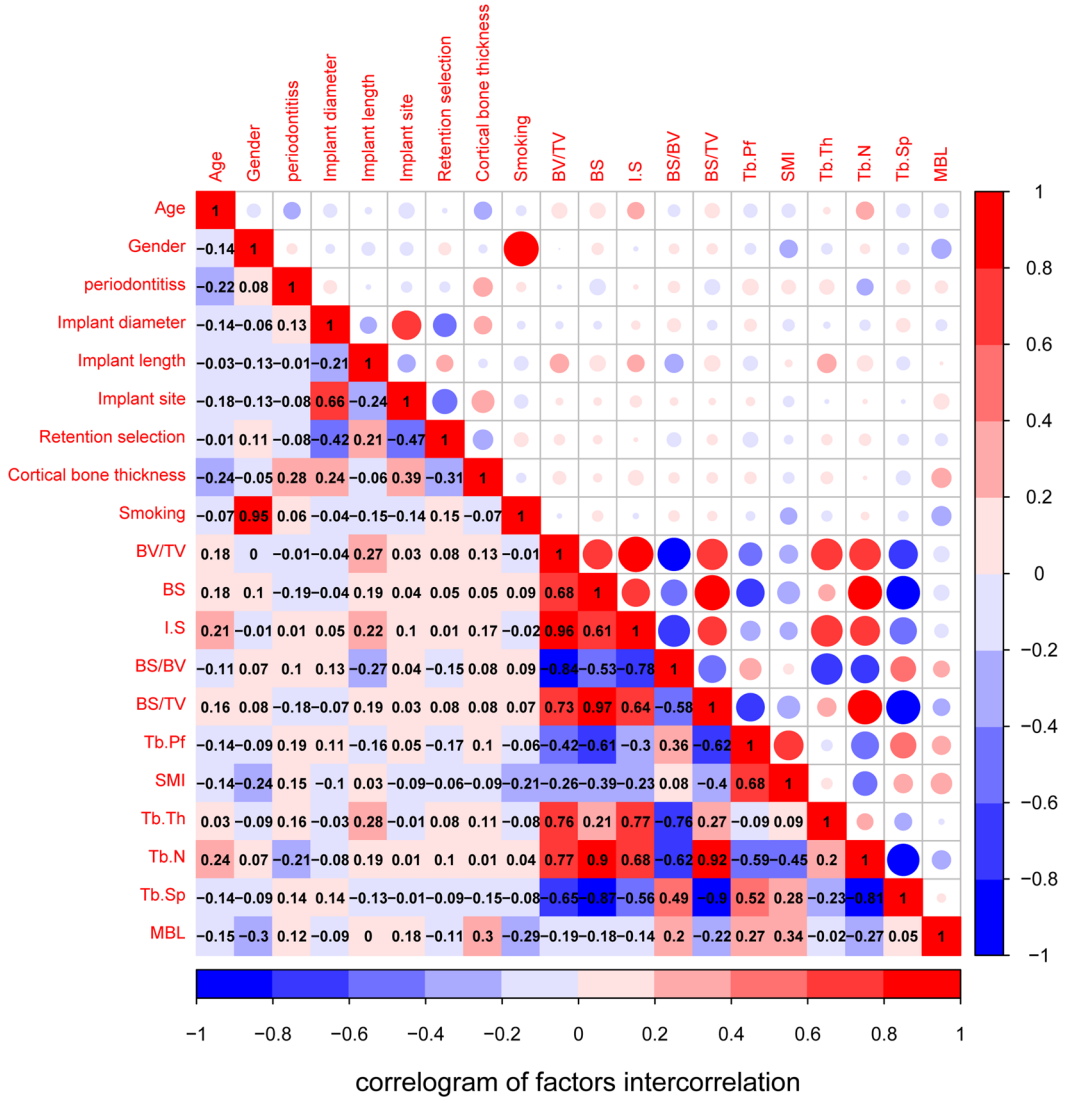

Figure 3. The visualization of correlation and covariance matrices between all variables. Red and blue represented positive and negative correlations, respectively. Darker colors indicated a more significant correlation.

in the peri-implant of severe MBL cases. However, in normal controls, Tb.N and BV/TV were superior to other morphological variables[11].

Although the current study has demonstrated that ML could predict the occurrence of MBL more effectively than conventional methods, some limitations need to be acknowledged. Due to the proximity of the measurement point to the implant root, implant artifacts remain unavoidable. The variables in the current study lacked results of the periodontal examination, such as probing depth. Additionally, this study was limited to patients who received implant treatment in mandible. Further studies on larger sample sizes using more relative variables (e.g. periodontal or microbiological) might be better for the ML performance. At last, a mean 20.95 ± 2.67 months of follow-up after functional loading was also limited to predict MBL. Hence, we entitled this study as a preliminary one.

In conclusion, the current study verified that the severity of early bone resorption was closely related to trabecular microarchitecture during the early stage of functional loading. Change of trabecular microarchitecture can provide an early warning for severe MBL. ML models SVM, ANN, LR, and RF indicate superior performance compared to the single predictor in predicting MBL of mandibular implant.

Methods

Study design. To address the research purpose, we designed and implemented a cross-sectional study. All subjects receiving implant treatment between January 2016 and March 2019 in the Department of Oral and Maxillofacial Surgery of Affiliated Stomatological Hospital of Nanjing Medical University were screened. The inclusion criteria of subjects were as follows: (1) above 18 years of age with good health; (2) having received fixed

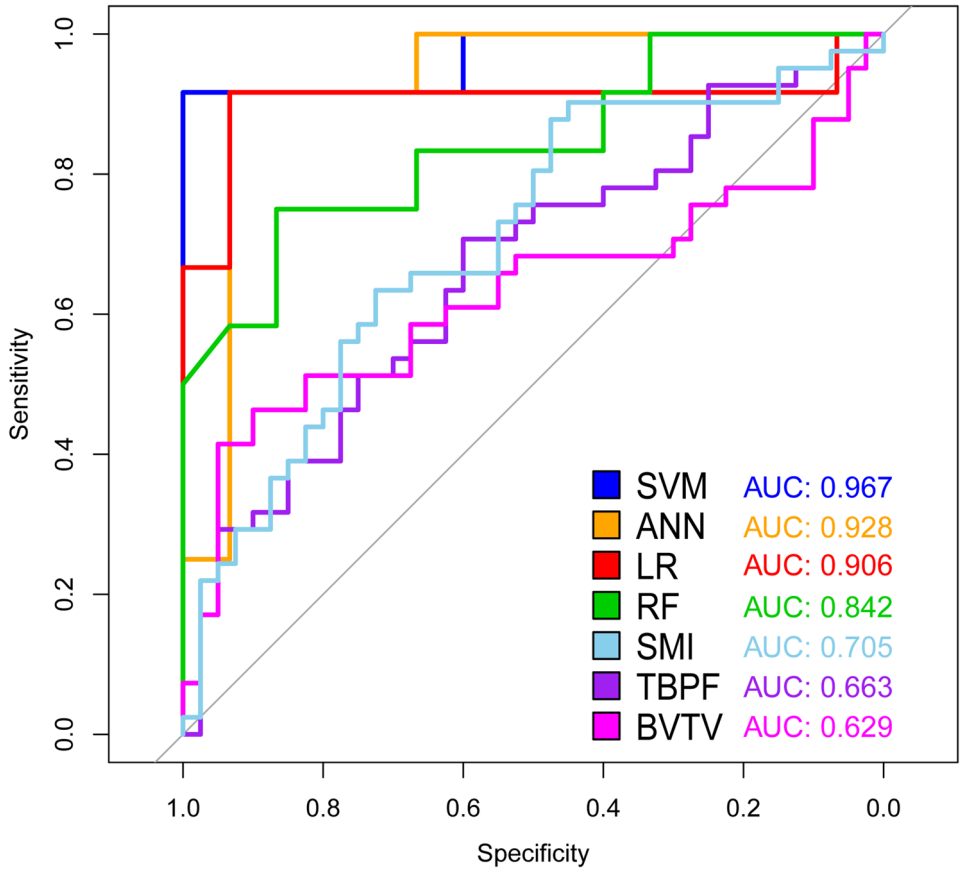

Figure 4. ROC & AUC of prediction models. The sensitivity and specificity of SVM, the best performing model, were 91.67% and 100.00%, respectively, at its optimal cutoff.

	ANN	LR	RF	SMI alone	Tb.Pf alone	BV/TV alone
	P-value	*P*-value	*P*-value	*P*-value	*P*-value	*P*-value
Support vector machine (SVM)	0.268	0.243	0.078	< 0.001***	< 0.001***	< 0.001***
Artificial neural network(ANN)		0.410	0.206	0.004**	< 0.001***	< 0.001***
Logistic regression (LR)			0.199	0.023*	0.009**	0.003**
Random forest (RF)				0.088	0.040*	0.018*
SMI alone					0.169	0.164
Tb.Pf alone						0.345

Table 1. Statistical significance of the difference between the areas under ROC curves. DeLong's test and Bootstrap test were used. *$P < 0.05$, **$P < 0.01$, ***$P < 0.001$.

prosthesis of the mandibular implant with at least 1 year of loading; (3) available integrated clinical data; (4) valid cone-beam computed tomography (CBCT) examination conducted at the following three time points: (T_0) preoperative bone assessment, (T_1) at the follow-up between 3 and 6 months after loading, and (T_2) at the follow-up above one year of post-loading. The exclusion criteria of subjects were as follows: (1) patients diagnosed with clinical or absolute failure based on the current guideline[4]; (2) patients with an incomplete periodontal follow-up examination and treatment record. (3) Patients receiving bone augmentation. Patients with smoking cessation for more than three months before surgical implant placement were taken as non-smokers.

This study was approved by the ethics committee of the Affiliated Stomatological Hospital of Nanjing Medical University (Approval number: PJ2019-038-001, Approval data: March 15, 2019) in accordance with the Helsinki Declaration II. Written informed consents were obtained from all participants.

Measurement of MBL. All subjects were examined by the CBCT (NewTom 5G cone-beam computed tomography device, QR s.r.l, Verona, Italy) at a reconstruct voxel size of 150 μm at the three time points. Scan-

Model	Sensitivity (%)	Specificity (%)	Optimal cutoff of probability	Positive predictive value	Negative predictive value	DLR positive	DLR negative	False positive	False negative	Optimal criterion
Support vector machine (SVM)	91.67	100.00	0.547	1.000	0.938	Infinite	0.083	0	1	0.917
Artificial neural network(ANN)	91.67	93.33	0.998	0.917	0.933	13.750	0.089	1	1	0.917
Logistic regression (LR)	91.67	93.33	0.824	0.917	0.933	13.750	0.089	1	1	0.917
Random forest (RF)	75.00	86.67	0.560	0.818	0.813	5.625	0.288	2	3	0.750
SMI alone	65.90	67.50	1.027	0.675	0.659	2.026	0.506	13	14	0.659
Tb.Pf alone	63.40	62.50	0.968	0.634	0.625	1.691	0.585	15	15	0.625
BV/TV alone	39.00	45.00	1.049	0.421	0.419	0.710	1.355	22	25	0.390

Table 2. Performance of each model at optimal cutoff point. The optimal cutoff was considered as the point maximizing the sum of sensitivity and specificity.

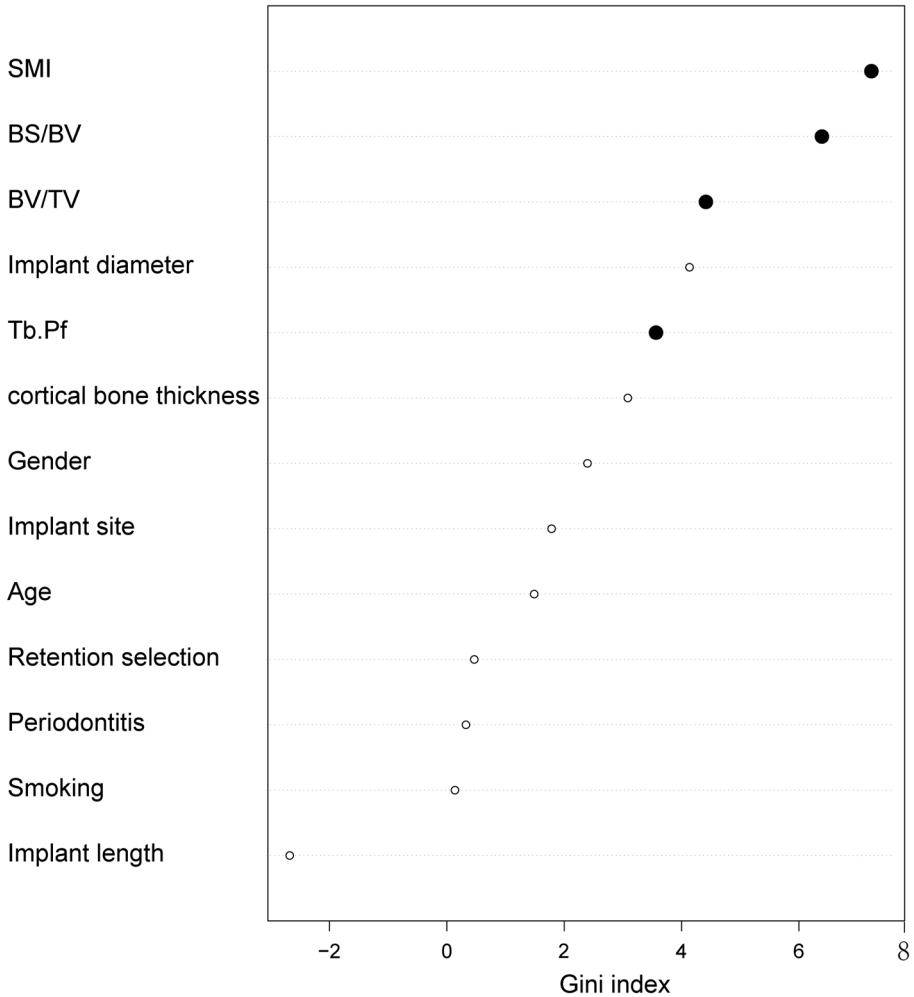

Figure 5. Variable importance plot of random forest model. The plot indicated the relative importance of the variables in the random forest model. Trabecular microarchitecture variables were marked as solid black points.

ning voltage and current were 110 kV and 10 mA, while exposure and scanning times were 3.6 s and 18 s. We reconstructed the original radiographs using the center of the implant in the sagittal, coronal, and transverse plane. The implant length and diameter were used to test the accuracy of reconstructed images. MBL measurement was performed as follows: (1) the horizontal interface between implant and abutment was validated as the reference loci; (2) vertical distances from the loci to the most coronal level of bone to implant contact at the

mesial and distal sites were measured at the preceding time points[27,28]; (3) analysis of radiographs was conducted by two investigators who did not participate in this study. We obtained the maximum MBL of the implant at T_1 and T_2 as the corresponding MBL level (Supplementary Fig. S1). According to the T_2 MBL level, we divided all subjects into two groups:

- *Normal controls* less than 2 mm MBL in the first year after fixed prosthesis, then less than 0.2 mm MBL per year
- *Severe MBL cases* MBL level exceeding normal controls

Measurement of peri-implant bone morphological parameters. We imported the T_1 radiographs to CT Analyzer (CTAn, SkyScan, Antwerpen, Belgium). The threshold value of binary selection was determined by completely distinguish cortical bone and trabecular bone (Supplementary Fig. S2a). We confirmed the region of interest (ROI) by the diameter of each implant. We selected five sequential ROI layers adjoining the implant root as the volume of interest (VOI) of peri-implant alveolar bone (Supplementary Fig. S2b). Another five sequential ROI layers away from the implant were chosen as VOI of the normal adjacent alveolar bone (Supplementary Fig. S2b). The trabecular bone morphological parameters, such as SMI, Tb.Pf, BV/TV, i.S, and Tb.N were extracted using three-dimensional analysis of each VOI. SMI, Tb.Pf, and i.S represent the shape and quality of trabecular bone. BV/TV and Tb.N usually mean quantity of trabecular bone. Finally, we calculated morphological variables by the ratio of peri-implant to normal adjacent alveolar bone.

PCA analysis. Including clinical and morphological parameters, all variables were utilized for ordination analysis and contribution degree evaluation of principle component using the "Multiple Factor Analysis" (MFA) function in the R package "FactoMineR". As a dimensionality reduction method, MFA reduces the complexity of multivariate data and allows visual interpretation of significant patterns. It is suited to data that contains both continuous and categorical variables. MFA also allows grouping of variables where each group is normalized individually to balance their influence. An MFA correlation circle plot depicts the continuous variables, and the factors plot depicts the categorical variables.

Visualization of correlation and covariance matrices. Correlation and covariance matrices can visualize the patterns and relationships between the variables. We had twenty original variables, including object variable MBL. The visualization of matrices re-ordered the variables in a correlation matrix and displayed the value by sign and magnitude. All iconic encodings in the matrix displayed the pattern and significance level of correlations between variables. The R package "corrgram" and "Hmisc" were employed in this study.

ML algorithms. Based on the R Programming Language (R Core Team, Vienna, Austria), four ML models, including SVM, ANN, LR model and RF, were constructed. The dataset was randomly split into two mutually exclusive sets, training (70%) and testing (30%), a method called holdout method[29]. LR model established with variable choice through backward elimination was implemented to assess risk factors and predict the diagnosis of diseases. The R package "e1071" was applied in the SVM model to accomplish regression and classification missions by constructing hyperplanes in a multidimensional space. SVM model could manage multiple continuous and categorical variables according to the decision plane. ANN model, a computerized encoding of artificial humanoid neuronal networks, included the input layer, hidden layers, and output layer. Neurons connected the adjacent layers as a medium for the delivery-feedback-correction-delivery cycle. This recursive process adjusted the weights for fewer errors and better accuracy. ANN model was implemented by R package "neural net". RF model, a ML algorithm based on the decision tree, could combine the output of a single decision tree to improve the overall performance. RF model was superior to a single decision tree in eliminating overfitting. RF model also could display the relative importance of the variables by the Gini index. We utilized the R package "randomForest" in the establishment of the RF model.

Statistical analysis. The chi-square test and Fisher's exact test were applied to compare the variables of severe MBL cases and normal controls. We utilized the Cochran-Armitage trend test for categorical variables, while continuous variables were assessed by Student's t-test and the Mann–Whitney rank-sum test. R programming language was used for all statistical analyses, while $P < 0.05$ was regarded as statistically significant.

Data availability

All CBCT files of patients and control subjects were stored in a non-public medical record database. CBCT data of the samples will not be shared.

Received: 16 June 2020; Accepted: 15 October 2020
Published online: 28 October 2020

References

1. Esposito, M., Hirsch, J. M., Lekholm, U. & Thomsen, P. Biological factors contributing to failures of osseointegrated oral implants. (I). Success criteria and epidemiology. *Eur. J. Oral Sci.* **106**, 527–551 (1998).
2. Esposito, M., Hirsch, J. M., Lekholm, U. & Thomsen, P. Biological factors contributing to failures of osseointegrated oral implants. (II). Etiopathogenesis. *Eur. J. Oral Sci.* **106**, 721–764 (1998).
3. Albrektsson, T., Zarb, G., Worthington, P. & Eriksson, A. R. The long-term efficacy of currently used dental implants—A review and proposed criteria of success. *Int. J. Oral Maxillofac. Implants* **1**, 11–25 (1986).

4. Misch, C. E. *et al.* Implant success, survival, and failure: The International Congress of Oral Implantologists (ICOI) Pisa Consensus Conference. *Implant Dent.* **17**, 5–15 (2008).
5. Papaspyridakos, P., Chen, C. J., Singh, M., Weber, H. P. & Gallucci, G. O. Success criteria in implant dentistry: A systematic review. *J. Dent. Res.* **91**, 242–248 (2012).
6. Duan, X. B. *et al.* Marginal bone loss around non-submerged implants is associated with salivary microbiome during bone healing. *Int. J. Oral Sci.* **9**, 95–103 (2017).
7. Derks, J. & Tomasi, C. Peri-implant health and disease. A systematic review of current epidemiology. *J. Clin. Periodontol.* **42**(Suppl 16), S158–S171 (2015).
8. Moy, P. K., Medina, D., Shetty, V. & Aghaloo, T. L. Dental implant failure rates and associated risk factors. *Int. J. Oral Maxillofac. Implants* **20**, 569–577 (2005).
9. Sener-Yamaner, I. D., Yamaner, G., Sertgoz, A., Canakci, C. F. & Ozcan, M. Marginal bone loss around early-loaded SLA and SLActive implants: Radiological follow-up evaluation up to 6.5 years. *Implant Dent.* **26**, 592–599 (2017).
10. Simons, W. F., De Smit, M., Duyck, J., Coucke, W. & Quirynen, M. The proportion of cancellous bone as predictive factor for early marginal bone loss around implants in the posterior part of the mandible. *Clin. Oral Implants Res.* **26**, 1051–1059 (2015).
11. Maquer, G., Musy, S. N., Wandel, J., Gross, T. & Zysset, P. K. Bone volume fraction and fabric anisotropy are better determinants of trabecular bone stiffness than other morphological variables. *J. Bone Miner. Res.* **30**, 1000–1008 (2015).
12. Zechner, W. *et al.* Radiologic follow-up of peri-implant bone loss around machine-surfaced and rough-surfaced interforaminal implants in the mandible functionally loaded for 3 to 7 years. *Int. J. Oral Maxillofac. Implants* **19**, 216–221 (2004).
13. Corcuera-Flores, J. R. *et al.* Relationship between osteoporosis and marginal bone loss in osseointegrated implants: A 2-year retrospective study. *J. Periodontol.* **87**, 14–20 (2016).
14. Levin, L., Hertzberg, R., Har-Nes, S. & Schwartz-Arad, D. Long-term marginal bone loss around single dental implants affected by current and past smoking habits. *Implant Dent.* **17**, 422–429 (2008).
15. Merheb, J. *et al.* Prediction of implant loss and marginal bone loss by analysis of dental panoramic radiographs. *Int. J. Oral Maxillofac. Implants.* **30**, 372–377 (2015).
16. Cruz, J. A. & Wishart, D. S. Applications of machine learning in cancer prediction and prognosis. *Cancer Inf.* **2**, 59–77 (2007).
17. Kourou, K., Exarchos, T. P., Exarchos, K. P., Karamouzis, M. V. & Fotiadis, D. I. Machine learning applications in cancer prognosis and prediction. *Comput. Struct. Biotechnol. J.* **13**, 8–17 (2015).
18. Kim, D. W., Kim, H., Nam, W., Kim, H. J. & Cha, I. H. Machine learning to predict the occurrence of bisphosphonate-related osteonecrosis of the jaw associated with dental extraction: A preliminary report. *Bone* **116**, 207–214 (2018).
19. McKinney, S. M. *et al.* International evaluation of an AI system for breast cancer screening. *Nature* **577**, 89–94 (2020).
20. Papantonopoulos, G., Gogos, C., Housos, E., Bountis, T. & Loos, B. G. Prediction of individual implant bone levels and the existence of implant "phenotypes". *Clin. Oral Implants Res.* **28**, 823–832 (2017).
21. Ha, S. R. *et al.* A pilot study using machine learning methods about factors influencing prognosis of dental implants. *J. Adv. Prosthodont.* **10**, 395–400 (2018).
22. Calvo-Guirado, J. L. *et al.* Marginal bone loss evaluation around immediate non-occlusal microthreaded implants placed in fresh extraction sockets in the maxilla: A 3-year study. *Clin. Oral Implants Res.* **26**, 761–767 (2015).
23. Kitamura, E., Stegaroiu, R., Nomura, S. & Miyakawa, O. Biomechanical aspects of marginal bone resorption around osseointegrated implants: Considerations based on a three-dimensional finite element analysis. *Clin. Oral Implants Res.* **15**, 401–412 (2004).
24. Di Fiore, A. *et al.* Influence of crown-to-implant ratio on long-term marginal bone loss around short implants. *Int. J. Oral Maxillofac. Implants* **34**, 992–998 (2019).
25. Karlsson, K. *et al.* Interventions for peri-implantitis and their effects on further bone loss: A retrospective analysis of a registry-based cohort. *J. Clin. Periodontol.* **46**, 872–879 (2019).
26. Chesnut, C. H. 3rd. *et al.* Effects of salmon calcitonin on trabecular microarchitecture as determined by magnetic resonance imaging: Results from the QUEST study. *J. Bone Miner. Res.* **20**, 1548–1561 (2005).
27. Zhang, X. X., Shi, J. Y., Gu, Y. X. & Lai, H. C. Long-term outcomes of early loading of straumann implant-supported fixed segmented bridgeworks in edentulous maxillae: A 10-year prospective study. *Clin. Implant Dent. Relat. Res.* **18**, 1227–1237 (2016).
28. Kumar, V. V., Sagheb, K., Kammerer, P. W., Al-Nawas, B. & Wagner, W. Retrospective clinical study of marginal bone level changes with two different screw-implant types: Comparison between tissue level (TE) and bone level (BL) implant. *J. Maxillofac. Oral Surg.* **13**, 259–266 (2014).
29. Kim, W. *et al.* Development of novel breast cancer recurrence prediction model using support vector machine. *J. Breast Cancer* **15**, 230–238 (2012).

Acknowledgments

We would like to thank our colleagues Shen Xin and Lin Jialing from Jiangsu Key Laboratory of Oral Diseases, Nanjing Medical University, for their support of radiographs analysis in this project.

Author contributions

The study was designed by H.Z. and H.J. The data was collected by H.Z. and analyzed by J.S. The ML models were built by H.Z., J.S. and X.C. The paper was written by H.Z. and revised by J.S., P.Z. and H.J. They all made great contributions to this study and should be listed as authors. All authors read and approved the manuscript.

Funding

This work was supported by the National Natural Science Foundation of China Grant (81771092), a project funded by the Priority Academic Program Development of Jiangsu Higher Education Institutions (PAPD, 2018-87), and Postgraduate Research & Practice Innovation Program of Jiangsu Province (KYCX19_1149).

Competing interests

The authors declare no competing interests.

Additional information

Supplementary information is available for this paper at https://doi.org/10.1038/s41598-020-75563-y.

Correspondence and requests for materials should be addressed to H.J.

Reprints and permissions information is available at www.nature.com/reprints.

Publisher's note Springer Nature remains neutral with regard to jurisdictional claims in published maps and institutional affiliations.